JACS
JOURNAL OF THE AMERICAN CHEMICAL SOCIETY

ARTICLE

pubs.acs.org/JACS

Potential-Dependent Recombination Kinetics of Photogenerated Electrons in n- and p-Type GaN Photoelectrodes Studied by Time-Resolved IR Absorption Spectroscopy

Akira Yamakata,*[,†] Masaaki Yoshida,[‡,#] Jun Kubota,[‡] Masatoshi Osawa,[§] and Kazunari Domen[‡]

[†]Graduate School of Engineering, Toyota Technological Institute, 2-12-1 Hisakata, Tempaku, Nagoya, 468-8511, Japan
[‡]Department of Chemical System Engineering, The University of Tokyo, 7-3-1 Hongo, Bunkyo-ku, Tokyo 113-8656, Japan
[§]Catalysis Research Center, Hokkaido University, N-21 W-10, Kita-ku, Sapporo 001-0021, Japan

ABSTRACT: Recombination kinetics of photogenerated electrons in n-type and p-type GaN photoelectrodes active for H_2 and O_2 evolution, respectively, from water was examined by time-resolved IR absorption (TR-IR) spectroscopy. Illumination of a GaN film with UV pulse (355 nm and 6 ns in duration) gives transient interference spectra in both transmittance and reflection modes. Simulation shows that the interference spectra are caused by photogenerated electrons. We observed that recombination in the microsecond region is greatly affected by the applied potentials, the lifetime becoming longer at negative and positive potentials for n- and p-type GaN electrodes, respectively. There is a good correlation between potential dependence of the steady-state reaction efficiency and that of the number of surviving electrons in the millisecond region. We also performed potential jump measurement to examine the shift in Fermi level by photogenerated charge carriers. In the case of n-type GaN, the electrode potential jumps to the negative side by accumulation of electrons in the bulk. However, in the case of p-type GaN, the electrode potential first jumps to the negative side within 20 μs and gradually shifts to the positive side in a few milliseconds, while the number of charge carriers is constant at >0.2 ms. This two-step process is ascribed to electron transport from the bulk to the surface of GaN, because the electrode potential is sensitive to the number of electrons in the bulk. The results confirm that TR-IR combined with potential jump measurement provides useful information for understanding the behavior of charge carriers in photoelectrochemical systems.

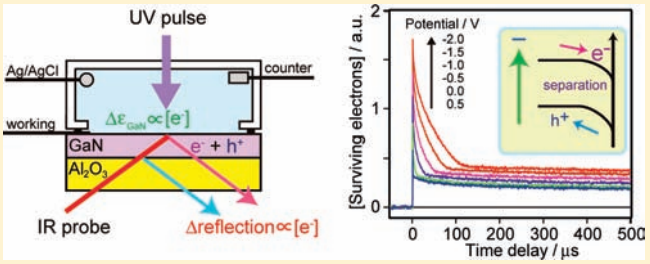

1. INTRODUCTION

Photocatalysts[1−6] and photoelectrodes[7−11] have attracted considerable attention due to their promising applications for storage of solar energy via chemical reactions. The efficiency of these semiconductor devices is determined by the behavior of charge carriers generated by band gap photoexcitation. In the case of photoelectrodes, it is well-known that reaction efficiency is greatly affected by the applied potential,[7−13] because the behavior of charge carriers depends on the applied potential. In semiconductor/electrolyte interfaces, the space charge layer plays an essential role in the behavior of charge carriers. Band-bending controls the charge separation between photogenerated electrons and holes. In the case of n-type semiconductors, applied positive potential enhances upward band bending, whereas downward band bending is enhanced at negative potentials on p-type semiconductors. Therefore, direct observation of the behavior of charge carriers under bias-voltage is essential for enhancing photoelectrochemical activities as well as for understanding the mechanism.

Transient optical spectroscopies, such as photoemission and absorption spectroscopies, provide information on the dynamics of photogenerated charge carriers. Time-resolved photoluminescence spectroscopy (TR-PL) has been widely used to study charge carrier dynamics on semiconductor quantum dots,[14] photocatalysts,[15] and photoelectrodes,[16] and it provides information on the lifetimes of photogenerated charge carriers and the energy of emitted light. However, the sensitivity of the TR-PL becomes lower when charge carriers are effectively separated, and it is insensitive to nonradiative decay, which is the dominant process for indirect semiconductors.[17,18] Transient absorption spectroscopy is sensitive to charge carriers, regardless of the recombination processes, radiative or nonradiative. Time-resolved IR absorption spectroscopy (TR-IR) is a powerful method for studying charge carrier dynamics in semiconductor materials[19,20] because the absorption coefficient of photogenerated electrons increases as the wavelength of the probe light becomes longer from visible to IR.[17,18] Furthermore, IR absorption is not disturbed by the emission of visible light during recombination. In previous studies, we have demonstrated that TR-IR enables study of photogenerated charge carrier dynamics such as recombination kinetics and charge transfer to reactant molecules (water, O_2,

Received: April 20, 2011
Published: June 17, 2011

MeOH) in TiO_2,[21,22] $NaTaO_3$,[23] and $BiWO_3$[24] photocatalysts. Short-lived reaction intermediates created by the charge transfer to reactant molecules[25] and electron transfer from a GaN photocatalyst to a Pt-cocatalyst,[26] an active center of hydrogen evolution, can also be examined by TR-IR.

In the present study, we used TR-IR to study charge carrier dynamics in photoelectrochemical systems. n- And p-type GaN thin film electrodes were used due to their activities for overall water splitting reaction under UV irradiation.[27−31] Recombination kinetics of photogenerated charge carriers under applied bias voltage was examined. The change in Fermi level by the accumulated charge carriers was also examined by transient potential jump measurement.[32,33]

2. EXPERIMENTAL SECTION

n-Type (2.9 μm in thickness, Si = 2×10^{17} cm^{-3}) and p-type (2 μm in thickness, Mg = 3×10^{19} cm^{-3}, [h] = 1.6×10^{17} cm^{-3}) GaN thin films epitaxially grown on a (0001)-oriented sapphire wafer (420 μm in thickness) were purchased from POWDEC Japan. Ohmic contact was made by depositing Au/Ti on n-type and Au/Ni alloy on p-type GaN in a vacuum. The electrolyte solution, 0.1 M Na_2SO_4 (pH = 6.5), was prepared from analytical grade Na_2SO_4 (Wako Chemicals, Tokyo) and Millipore water (>18 MΩ), and it was deaerated with Ar gas before use. The photoelectrochemical cell used was a three-electrode glass cell with a flat Pyrex optical window for introducing pump light. Potential was controlled and measured against an Ag/AgCl (sat. KCl) electrode [E(AgCl/Ag) = +0.197 V vs NHE at 25 °C)] with a homemade potentiostat that has a fast voltage follower (~1 ns).[33] The counter electrode was a Pt mesh.

The electrode was illuminated with the third harmonic output from a Continuum Surelite-I Nd:YAG pulse laser (355 nm, 6 ns in duration, 10 Hz in repetition rate) at the normal incidence, and the changes in IR absorption (ΔAbs) on the electrode and open circuit potential E_i caused by the laser pulses were recorded as a function of time with a digital oscilloscope (Iwatsu, DS-4262). The diameter of UV pulse was expanded to be 30 mm, which is large enough for the IR beam (5 mm) and the GaN sample (20 mm). The laser power (0.5 mJ cm^{-2}) is weak enough to avoid damage on the GaN sample. For measuring ΔAbs and E_i, the counter electrode was mechanically disconnected from the potentiostat 2 ms before the laser irradiation and reconnected 10 ms later by using an electromagnetic microrelay (Omron, G5V) and a function generator (NF circuit, WF1973) synchronized with the laser irradiation. The disconnection is indispensable to prevent charge flow from the electrode to the external circuit and potential modification by the feed-back circuit of the potentiostat.[33]

The time-resolved IR absorption study was performed by using a homemade TR-IR spectrometer.[34] Briefly, the IR light emitted from an $MoSi_2$ coil was focused on the sample, and transmitted or reflected light was detected with a photovoltaic MCT detector (Kolmar) after being monochromatized by a dispersive spectrometer (Acton SP-2300i). The time-resolution of this spectrometer is limited to ~50 ns, the time response of the MCT detector

Potential-dependent oxidation and reduction of water on n- and p-type GaN electrodes were measured during a potential sweep at 20 mV s^{-1} with illumination of UV light from an LED lamp (365 nm, Omron, ZUV-C20H) at intervals of 2 s.

3. RESULTS AND DISCUSSION

3.1. Photoelectrochemical Reactions of Water on n- and p-Type GaN Photoelectrodes. First, steady-state reactions of water on n- and p-type GaN photoelectrodes were studied under applied potential. The photocurrent for the n-type GaN electrode

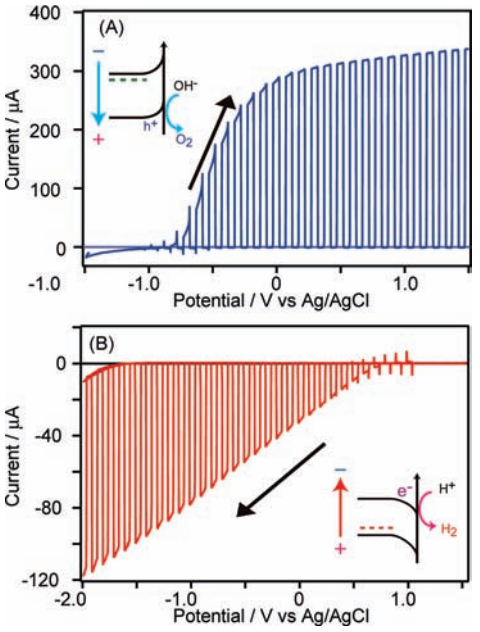

Figure 1. Potential-dependent photocurrent on n-type (A) and p-type (B) GaN electrodes irradiated by 365 nm UV light (3 mW cm^{-2}) in 0.1 M Na_2SO_4 (pH = 6.5) during a potential sweep at 20 mV s^{-1}. The electrode potentials were referenced to Ag/AgCl (sat. KCl). The electrodes were irradiated at intervals of 2 s. These photocurrents are due to oxidation and reduction of water on n- and p-type GaN, respectively.

measured in 0.1 M Na_2SO_4 during a positive potential sweep from −1.5 to 1.5 V vs Ag/AgCl is shown in Figure 1A. Anodic current arising from the oxidation of water to produce O_2 by photogenerated holes[27,31] flows above −0.8 V under UV illumination. The amplitude of the oxidation current becomes larger as the potential becomes more positive. The results obtained for the p-type GaN electrode were the opposite of those for the n-type GaN, as shown in Figure 1B, where the photoinduced cathodic current is observed below 0.7 V. This current is ascribed to the reduction of water to produce H_2 by photogenerated electrons.[28,30] The amplitude of this reduction current becomes larger as the electrode potential becomes more negative, suggesting that the efficiency of the reduction is enhanced at negative potentials. These results are consistent with the results of previous studies performed on n-[27,31] and p-type[28,30] GaN.

n- And p-type GaN electrodes show opposite potential dependence of the photocurrent: only oxidation and reduction proceed on each sample, and their reaction efficiencies are enhanced at positive and negative potentials, respectively. This opposite potential dependence is ascribed to different directions of the band bending at the liquid/solid interfaces, as shown in the inset of Figure 1A,B. Since these photoelectrochemical reactions are induced by photogenerated charge carriers, the reaction efficiency should be related to the number of charge carriers that can escape from the recombination. In the following sections, we discuss the potential-dependent recombination kinetics of these charge carriers on n- and p-type GaN electrodes.

3.2. Time-Resolved IR Absorption Study of Photogenerated Electrons on GaN Thin Film. The optical response of GaN thin film induced by the band gap photoexcitation was examined by using TR-IR with transmission and reflection modes. Figure 2A shows transient IR absorption spectra of n-type GaN irradiated by 355-nm UV pulses that were measured in air with the transmission

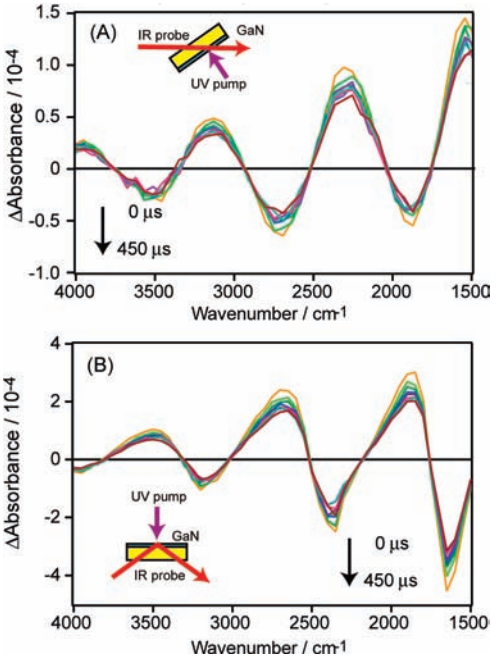

Figure 2. Time-resolved IR absorption spectra of the n-type GaN electrode irradiated by 355 nm laser pulses (6 ns in duration, 0.5 mJ cm^{-2}). Ten spectra measured from 0 to 450 μs at every 50 μs step are shown. The spectra were measured in air with transmission (A) and reflection (B) modes. The spectral resolution is 32 cm^{-1} and the incident angle of IR light is 60° from the surface normal.

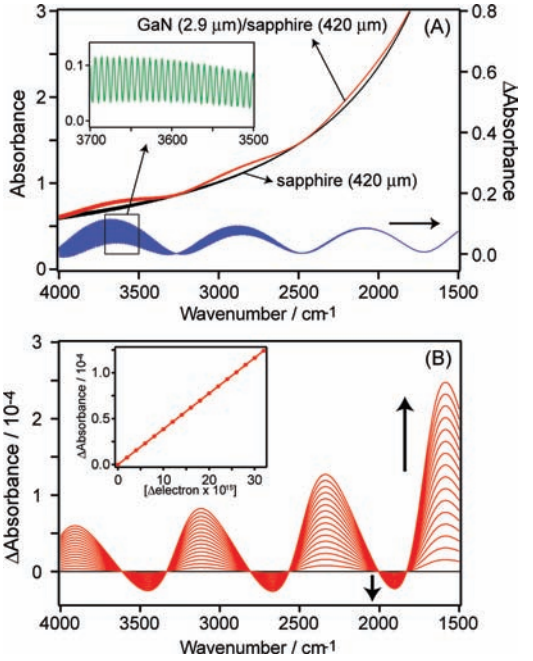

Figure 3. (A) Simulated transmission IR spectra of sapphire (420 μm in thickness) and n-type GaN (2.9 μm in thickness, $n = 2.0 \times 10^{17}$ cm^{-3})/sapphire in air at the incident angle of 60° from the surface normal. The difference spectrum of GaN/sapphire is also shown. (B) Difference IR spectra for the increase in electron density in the n-type GaN/sapphire system from $n = 2.00$ to 2.32×10^{17} cm^{-3} at every 2×10^{15} cm^{-3} step. The spectra are weight-averaged for comparison with results of experiments performed with the resolution of 32 cm^{-1}. The inset shows the absorbance change at 2300 cm^{-1} arising from the increase in electron density from $n = 2.00 \times 10^{17}$ cm^{-3}.

mode. The sample was irradiated by UV pulses from the surface normal, and the IR light was illuminated at the incident angle of 60°. The results show that the absorbance changes periodically. The amplitude of the oscillation increases at lower wavenumbers. The shape of the spectra does not change with delay time from the UV irradiation, and only the amplitude decreases. A similar oscillatory pattern is observed with the reflection mode (Figure 2B), but the peaks are opposite to those observed with the transmittance mode. The results suggest that these oscillations are due to the interference effect by the multiple reflection of IR light in the thin GaN film.

In order to confirm the interference effect, we simulated transmission and reflection IR spectra of a thin (2.9 μm) GaN layer epitaxially grown on a 420-μm-thick (0001)-oriented sapphire substrate. The dielectric constant of n-type GaN at frequency ω in the infrared region is given by

$$\varepsilon_{GaN}(\omega) = \varepsilon_\infty - \frac{{\omega_p}^2}{\omega(\omega + i\gamma)} + \frac{S{\omega_0}^2}{{\omega_0}^2 - \omega^2 - i\omega\Gamma} \quad (1)$$

where the first term is the dielectric constant at high frequency limit, and the second and third terms represent contributions of the free carriers and the lattice vibration (phonon), respectively.[35] In the second term, γ is the carrier collision frequency, and the plasma frequency of the free carriers, ω_p, is given by

$$\omega_p(n)^2 = \frac{ne^2}{m_e^* \varepsilon_\infty \varepsilon_0} \quad (2)$$

where n is the carrier concentration, e and m_e^* are the charge and effective mass of electrons (=0.2 m[36]), respectively, and ε_0 is the permittivity of vacuum. The empirical dielectric function of sapphire has also been reported in the literature.[37] The optical responses of both GaN and sapphire are anisotropic; i.e., the parameter values for the electric fields parallel and perpendicular to the c-axis (which is perpendicular to the sample plane) are different. The anisotropy was taken into account in the calculation by using the method developed by Hasegawa et al.[38]

A transmission spectrum of the GaN/sapphire system calculated by assuming $n = 2 \times 10^{17}$ cm^{-3} is shown in Figure 3A by the red trace. From a comparison with the transmission spectrum of the sapphire substrate (black trace), two interference fringes with different peak separations (~7 and ~800 cm^{-1}) are found. The coarse fringe becomes clearer by subtracting the absorption by the substrate (blue trace). The fine and coarse fringes apparently arise from the interferences of light in the substrate and in the GaN overlayer, respectively. The amplitude of the fine fringe becomes smaller at lower frequencies due to the larger absorption of sapphire at lower frequencies. The peak separation of the calculated coarse fringe is the same as that observed (Figure 2), but the positions of the peaks are different.

By assuming that n is increased by the UV radiation, we also calculated the spectra for different values of n. Figure 3B shows difference spectra for increasing n from 2.0×10^{17} to 2.32×10^{17} cm^{-3} at every 2×10^{15} cm^{-3} step, where the fine interference fringe arising from the sapphire substrate was removed by taking a weight average for a comparison with the results of experiments performed with the spectral resolution of 32 cm^{-1}. The calculated difference spectra are almost identical to those shown in Figure 2A except for a relatively large peak around 1500 cm^{-1},

dx.doi.org/10.1021/ja203639q |J. Am. Chem. Soc. 2011, 133, 11351–11357

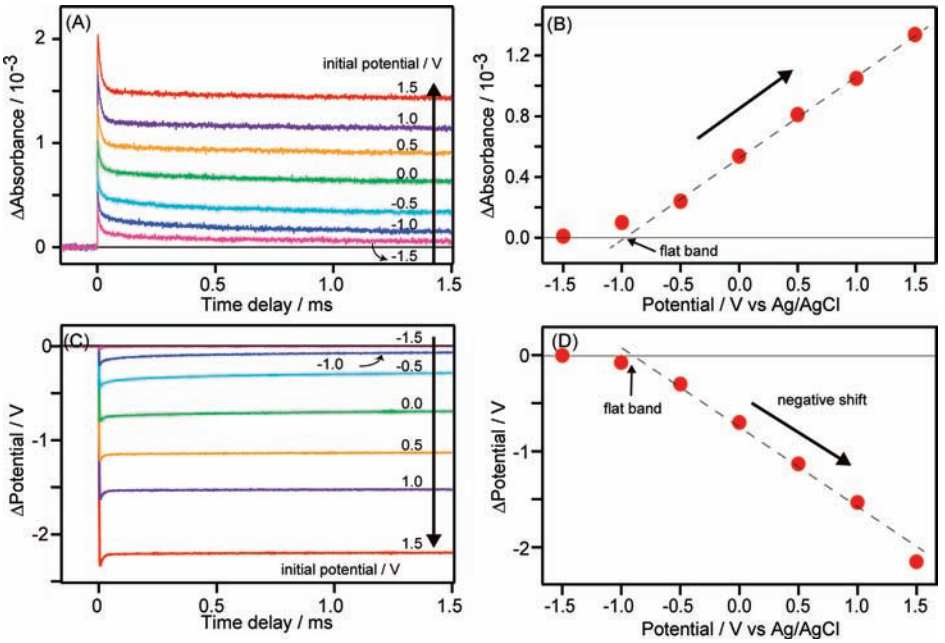

Figure 4. (A) Initial potential dependence of transient IR reflection of the n-type GaN electrode at 1950 cm^{-1} triggered by 355 nm laser pulse (6 ns in duration, 0.5 mJ cm^{-2}) irradiation. The curves were obtained at the initial potentials as indicated in the figure. These experiments were performed in 0.1 M Na_2SO_4 (pH = 6.5) and the electrode potentials were referenced to Ag/AgCl (sat. KCl). (B) Amplitude of transient IR absorption at 1 ms. (C) Initial potential dependence of the potential jump induced by 355 nm laser pulse (6 ns in duration, 0.5 mJ cm^{-2}) irradiation on the n-type GaN electrode. (D) Amplitude of transient potential shift obtained at 1 ms.

which is probably due to overestimation of the third term in eq 1 (The parameter values for GaN used in the calculation are for $n \sim 10^{19}$ cm^{-3} [35]). Careful inspection reveals that the maxima and minima of the oscillatory patterns in the difference spectra are located midway between the minima and maxima and midway between the maxima and minima, respectively, in the interference fringe shown in Figure 3A. Such a pattern is generated by the shift of the interference fringe. It should be noted that the photoinduced change in the refractive index ($Re(\sqrt{\varepsilon_{GaN}(\omega)})$) is very small, and hence, the shift in the fringe also is very small. Therefore, we can conclude that the change in photogenerated charge carrier density is reflected in the observed oscillatory patterns in Figure 2 and that the measurement of the transmission or reflection difference with and without UV radiation employed in the present study is a very sensitive way to examine photogenerated charge carriers. It is also notable that peak intensities in the difference spectra are proportional to n as shown in the inset of Figure 3B, which enables us to estimate the amount of photogenerated charge carriers. The results obtained with the reflection mode were also simulated in the same way (data not shown).

According to the Drude model, both electrons and holes affect the transient IR spectra, and their contribution becomes larger as the effective mass becomes smaller (eq 2). The effective masses of electrons and holes in GaN are 0.20[36] and 2.2,[39] respectively. Therefore, photogenerated electrons mainly contribute to the reflectivity changes. We previously reported that photogenerated electrons in photocatalysts such as TiO_2[21,25,34] and $NaTaO_3$[23] give structureless strong IR absorption with increase in the intensity at lower frequencies.[17,18] In the present study, the IR absorption by photogenerated electrons was not clearly separated due to the strong amplitude of the oscillation. Regardless of the origin of the transient IR response, both contributions similarly affect the transient IR signal and we can therefore concentrate on the study of decay kinetics of photogenerated electrons by observing the change in IR intensity at a fixed wavenumber.

3.3. Dynamics of Photogenerated Charge Carriers in n-Type GaN. We then studied the recombination kinetics of photogenerated electrons under electrochemical conditions by TR-IR. To avoid strong IR absorption by the aqueous electrolyte, measurements were performed with the reflection mode. Figure 4A shows the change in IR reflection of the n-type GaN electrode irradiated by UV pulses, which is ascribed to the change of dielectric constant of GaN by the photogenerated electrons. The results show that the intensity of reflected IR light at 1950 cm^{-1} becomes smaller due to the band gap photoexcitation. The decay of the transient IR intensity consists of at least two components of different lifetimes: one recovers within 100 μs and the other does not decay at all in the ms region. It is evident that the number of surviving electrons in the millisecond region becomes larger as the applied potential becomes more positive from −1.5 to 1.5 V. The transient IR signal at 1 ms is plotted as a function of applied potential (Figure 4B). The number of surviving electrons increases almost linearly as the applied potential becomes more positive with intersection of the x-axis at −0.9 V. This x-intercept potential corresponds to the flat band potential of n-type GaN, which is reported in previous papers.[27,28,40] At potentials more positive than the flat band potential, upward band bending is enhanced where electrons and holes are forced to move into the bulk and to the surface, respectively. Therefore, the charge carriers are effectively separated at positive potentials, and hence, the number of photogenerated electron is increased.

This potential-dependent charge separation in n-type GaN is consistent with results obtained by steady-state PL measurements.[40]

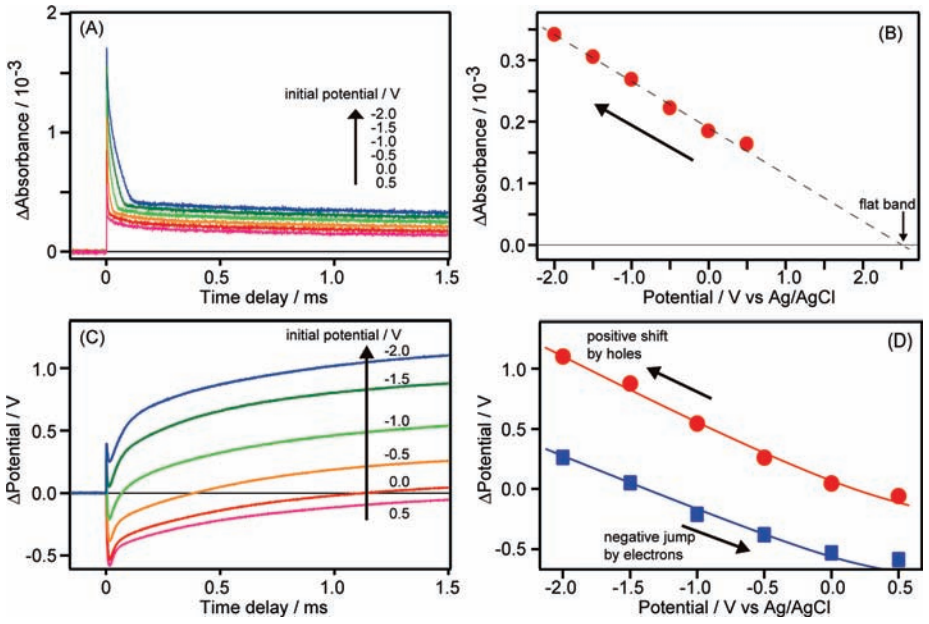

Figure 5. (A) Initial potential dependence of transient IR reflection of the p-type GaN electrode at 2050 cm^{-1} triggered by 355 nm laser pulse (6 ns in duration, 0.5 mJ cm^{-2}) irradiation. The curves were obtained at the initial potentials as indicated in the figure. These experiments were performed in 0.1 M Na_2SO_4 (pH = 6.5) and the electrode potentials were referenced to Ag/AgCl (sat. KCl). (B) Amplitude of transient IR absorption at 1 ms. (C) Initial potential dependence of the potential jump induced by 355 nm laser pulse (6 ns in duration, 0.5 mJ cm^{-2}) irradiation on the p-type GaN electrode. (D) Amplitude of transient potential jump at 10 μs (blue trace) and potential shift at 1.5 ms (red trace).

It has been shown that PL intensity becomes larger as the applied potential becomes more positive than the flat band potential, suggesting that radiative recombination is effectively suppressed at higher potentials, although PL measurement does not give information about time-dependent carrier dynamics. It is notable that photogenerated electrons do not decay in the millisecond domain. This extremely long lifetime of electrons would be due to the complete separation of electrons and holes via the potential gradient at the space charge layer. We have reported that both of the electron- and hole-consuming reactions of water affect the decay kinetics of photogenerated electrons.[21−23] However, when electrons and holes are completely separated, the hole-consuming reaction no longer affects the decay of electrons. In the case of n-type GaN, holes should be consumed by water; however, it is not clear from Figure 4A if holes are consumed or not by water due to the insensitivity of holes to TR-IR. Multielectron injection from the reactants into GaN, which is often observed during photooxidation, could be excluded, because the signal intensity does not increase.

The photogenerated charge carriers also cause a change in the Fermi level of GaN, resulting in a change in the electrode potential. Figure 4C shows the transient change in electrode potential induced by the UV pulse irradiation. The results show that the electrode potential jumps to the negative side and recovers with time delay. There are at least two components of different lifetimes, one component recovering within 100 μs and the other not decaying at all in the millisecond region. This negative potential change suggests that the Fermi level becomes higher with irradiation. The amplitude of the negative potential shift becomes larger as the applied potential becomes more positive. This negative potential shift is due to the increase in the Fermi level of GaN caused by accumulation of electrons in the conduction band of the electrode. Figure 4D shows the amplitude of the potential shift at 1 ms, suggesting that the amplitude increases as the initial potential becomes more negative than the flat band potential. This potential jump measurement is comparable with the results of TR-IR measurements (Figure 4B) showing that the number of accumulated electrons increases at positive potentials. In the case of n-type GaN, it can be concluded that TR-IR and potential jump measurements give consistent results regarding the behavior of photogenerated electrons in photoelectrochemical systems.

3.4. Dynamics of Photogenerated Charge Carriers in p-Type GaN. We examined the behavior of photogenerated charge carriers in the p-type GaN electrode, because p-type semiconductors show potential dependence opposite to that of n-type semiconductors. Figure 5A shows the change in IR reflection of p-type GaN at 2050 cm^{-1} induced by UV pulse irradiation. Similar results with n-type GaN were obtained by irradiation, with the transient signal gradually recovering with time delay: there are at least two components of different lifetimes, one recovering within 100 μs and the other not decaying at all in the millisecond region. However, the direction of potential dependence is opposite from that of n-GaN: the rate of recombination within 100 μs becomes longer and the number of surviving electrons at 1.5 ms (Figure 5B) linearly increases as the potential becomes more negative with intersection of the x-axis at 2.6 V. This x-intercept potential corresponds to the flat band potential of p-type GaN as reported in previous papers.[28,30] This opposite potential dependence from n-type GaN is ascribed to the opposite band bending.

In the time region performed in this work (0−1.5 ms), acceleration of electron decay due to the electron-consuming reaction by water was not observed, although electrons should be consumed by water on p-type GaN. This result suggests that the rate of electron-consuming reaction of water is slower than 1.5 ms on bare GaN. It has been reported that the loading of CrO_x/Rh[29] and Pt[26] cocatalysts greatly enhances the reduction of water on GaN. We have reported that electron-consuming reactions on TiO_2[21] and $NaTaO_3$[23] are accelerated from the subseconds

dx.doi.org/10.1021/ja203639q |J. Am. Chem. Soc. 2011, 133, 11351–11357

region to microseconds region by loading Pt and NiO cocatalysts. This should also be the case on the bare GaN surface.[26] In addition, it was clearly shown that most of the charge carriers are recombined within 100 μs. This accelerated recombination would be due to defects created by doped Mg^{2+}. It is well-known that most of the doped Mg^{2+} is deactivated by the formation of neutral Mg−H complexes.[41] In this sample, only ∼0.5% (1.6×10^{17} cm^{-3}/3.0×10^{19} cm^{-3}) of doped Mg^{2+} works as an acceptor, while Si works as a donor at ∼100% efficiency in the case of n-type GaN. These results suggest that the reaction efficiency could be further enhanced by developing more efficient p-doping.

The change in Fermi level was also examined by potential jump measurement. Figure 5C shows the results for p-GaN induced by band gap photoexcitation. The electrode potential first jumped to the negative side and slowly shifted to the positive side in a few ms. The temporal profiles of these potential jumps are totally different from that observed on n-GaN (Figure 4B). We propose that these complex potential changes are due to the redistribution of photogenerated charge carriers between the bulk and surface, because potential measurement is sensitive to changes in the Fermi level of bulk. Just after the irradiation, electrons and holes are generated both in the bulk and the surface. Regardless of the existence of holes in the bulk, the Fermi level of the bulk becomes higher due to electrons in the conduction band of the bulk. However, the photogenerated electrons in the bulk migrate to the surface with time delay. Complete migration of the electrons to the interface gradually decreases the Fermi level of the bulk, and holes that have accumulated in the bulk further decrease the Fermi level to shift the potential toward the positive side. The slow process of positive potential shift suggests that it takes a few milliseconds for complete migration of the electrons from the bulk to the surface. The TR-IR measurement (Figure 5A) shows that the number of photogenerated electrons is constant from 0.2 to 1.5 ms; however, the redistribution of charge carriers via the space charge layer causes a great change in the Fermi level of the bulk. Figure 5D shows the amplitudes of the negative potential shift (at 20 μs) and positive potential shift (at 1.5 ms). As the initial potential becomes positive, the amplitude of the negative potential jump becomes larger (blue trace), suggesting that the number of electrons remaining in the bulk is larger due to insufficient downward band bending. However, in the case of positive potential shift, the amplitude becomes larger at negative potentials (red trace), where downward band bending is enhanced. The amplitude of the potential changes well reflects the number of charge carriers in the bulk.

4. CONCLUSION

In this work, we demonstrated the feasibility of time-resolved IR absorption spectroscopy for studying the potential-dependent recombination kinetics of photogenerated charge carriers in a semiconductor photoelectrochemical system. TR-IR enables study of the recombination kinetics because electrons generated in semiconductors change the reflectivity of the IR light. The reflection mode prevents strong IR absorption by bulk water. We applied this method to study the potential-dependent recombination kinetics in n- and p-type GaN, which are known to generate O_2 and H_2 from water, respectively. In the case of n-type GaN, oxidation of water is enhanced at positive potentials. We observed that the number of surviving electrons is increased as the applied potential becomes more positive. In the case of p-type GaN, on the other hand, reduction of water is enhanced at more negative potentials. We observed that the number of photogenerated electrons is also increased as the potential becomes more negative. These results confirm that the potential-dependent lifetime of the charge carriers is responsible for the potential-dependent activities of water splitting reactions. Potential jump measurement gives additional information about the behavior of photogenerated charge carriers, i.e., the change in Fermi level in the bulk. In the case of n-type GaN, the electrode potential becomes negative due to the increase in Fermi level by the accumulated electrons. The temporal profiles of the TR-IR signal and the potential change are almost identical. However, in the case of p-type GaN, the potential jumps to the negative side first and then slowly shifts to the positive side. This two-step potential jump is responsible for the complex charge redistribution between the bulk and surface, in which electrons generated in the bulk increases the Fermi level in the bulk and the following migration of electrons toward the surface decreases the Fermi level in the bulk. During the redistribution of these charge carriers, their number remains constant, as confirmed by TR-IR measurements. Therefore, combined TR-IR and potential jump measurement is useful for understanding the behavior of photogenerated charge carriers. Since the efficiency of photoelectrochemical systems is governed by the behaviors of photogenerated charge carriers, this method brings useful information to develop more efficient reaction systems.

AUTHOR INFORMATION

Corresponding Author

yamakata@toyota-ti.ac.jp

Present Addresses

[#]Department of Chemistry, Faculty of Science and Technology, Keio University, 3-14-1 Hiyoshi, Kohoku-ku, Yokohama 223-8522, Japan.

ACKNOWLEDGMENT

This work was partly supported by MEXT of Japan (Basic Research (B) No. 23360360 and Priority Areas 477 and 470). We are grateful to POWDEC Japan for preparing Au/Ni alloy electrode on p-type GaN and technical advice.

REFERENCES

(1) Linsebigler, A. L.; Lu, G. Q.; Yates, J. T. *Chem. Rev.* **1995**, *95*, 735.
(2) Thompson, T. L.; Yates, J. T. *Chem. Rev.* **2006**, *106*, 4428.
(3) Hoertz, P. G.; Mallouk, T. E. *Inorg. Chem.* **2005**, *44*, 6828.
(4) Maeda, K.; Domen, K. *J. Phys. Chem. C* **2007**, *111*, 7851.
(5) Kudo, A.; Miseki, Y. *Chem. Soc. Rev.* **2009**, *38*, 253.
(6) Inoue, Y. *Energy Environ. Sci.* **2009**, *2*, 364.
(7) Kamat, P. V. *Chem. Rev.* **1993**, *93*, 267.
(8) Nozik, A. J.; Memming, R. *J. Phys. Chem.* **1996**, *100*, 13061.
(9) Lewis, N. S. *J. Phys. Chem. B* **1998**, *102*, 4843.
(10) Hagfeldt, A.; Gratzel, M. *Chem. Rev.* **1995**, *95*, 49.
(11) Koval, C. A.; Howard, J. N. *Chem. Rev.* **1992**, *92*, 411.
(12) Cowan, A. J.; Tang, J. W.; Leng, W. H.; Durrant, J. R.; Klug, D. R. *J. Phys. Chem. C* **2010**, *114*, 4208.
(13) Pendlebury, S. R.; Barroso, M.; Cowan, A. J.; Sivula, K.; Tang, J. W.; Gratzel, M.; Klug, D.; Durrant, J. R. *Chem. Commun.* **2011**, *47*, 716.
(14) Yoffe, A. D. *Adv. Phys.* **2001**, *50*, 1.
(15) Blasse, G. *Prog. Solid State Chem.* **1988**, *18*, 79.
(16) Kauffman, J. F.; Balko, B. A.; Richmond, G. L. *J. Phys. Chem.* **1992**, *96*, 6371.

(17) Pankove, J. I. *Optical Processes in Semiconductors*; Dover: New York, 1975.
(18) Basu, P. K. *Theory of Optical Processes in Semiconductors*; Oxford University Press: New York, 1997.
(19) Skinner, D. E.; Colombo, D. P.; Cavaleri, J. J.; Bowman, R. M. *J. Phys. Chem.* **1995**, *99*, 7853.
(20) Heimer, T. A.; Heilweil, E. J. *J. Phys. Chem. B* **1997**, *101*, 10990.
(21) Yamakata, A.; Ishibashi, T.; Onishi, H. *J. Phys. Chem. B* **2001**, *105*, 7258.
(22) Yamakata, A.; Ishibashi, T. A.; Onishi, J. *J. Phys. Chem. B* **2003**, *107*, 9820.
(23) Yamakata, A.; Ishibashi, T.; Kato, H.; Kudo, A.; Onishi, H. *J. Phys. Chem. B* **2003**, *107*, 14383.
(24) Amano, F.; Yamakata, A.; Nogami, K.; Osawa, M.; Ohtani, B. *J. Am. Chem. Soc.* **2008**, *130*, 17650.
(25) Yamakata, A.; Ishibashi, T.; Onishi, H. *Chem. Phys. Lett.* **2003**, *376*, 576.
(26) Yoshida, M.; Yamakata, A.; Takanabe, K.; Kubota, J.; Osawa, M.; Domen, K. *J. Am. Chem. Soc.* **2009**, *131*, 13218.
(27) Fujii, K.; Karasawa, T. K.; Ohkawa, K. *Jpn. J. Appl. Phys. 2* **2005**, *44*, L543.
(28) Fujii, K.; Ohkawa, K. *Jpn. J. Appl. Phys. 2* **2005**, *44*, L909.
(29) Maeda, K.; Teramura, K.; Saito, N.; Inoue, Y.; Domen, K. *Bull. Chem. Soc. Jpn.* **2007**, *80*, 1004.
(30) Kobayashi, N.; Narumi, T.; Morita, R. *Jpn. J. Appl. Phys. 2* **2005**, *44*, L784.
(31) Ono, M.; Fujii, K.; Ito, T.; Iwaki, Y.; Hirako, A.; Yao, T.; Ohkawa, K. *J. Chem. Phys.* **2007**, *126*, 7.
(32) Yamakata, A.; Uchida, T.; Kubota, J.; Osawa, M. *J. Phys. Chem. B* **2006**, *110*, 6423.
(33) Yamakata, A.; Osawa, M. *J. Phys. Chem. C* **2008**, *112*, 11427.
(34) Yamakata, A.; Ishibashi, T.; Onishi, H. *Chem. Phys. Lett.* **2001**, *333*, 271.
(35) Barker, A. S.; Ilegems, M. *Phys. Rev. B* **1973**, *7*, 743.
(36) Pearton, S. J.; Abernathy, C. R.; Overberg, M. E.; Thaler, G. T.; Norton, D. P.; Theodoropoulou, N.; Hebard, A. F.; Park, Y. D.; Ren, F.; Kim, J.; Boatner, L. A. *J. Appl. Phys.* **2003**, *93*, 1.
(37) Harman, A. K.; Ninomiya, S.; Adachi, S.; Phys., J. A. *J. Appl. Phys.* **1994**, *76*, 8032.
(38) Hasegawa, T.; Takeda, S.; Kawaguchi, A.; Umemura, J. *Langmuir* **1995**, *11*, 1236.
(39) Im, J. S.; Moritz, A.; Steuber, F.; Harle, V.; Scholz, F.; Hangleiter, A. *Appl. Phys. Lett.* **1997**, *70*, 631.
(40) Harvey, E.; Heffernan, C.; Buckley, D. N.; O'Raifeartaigh, C. *Appl. Phys. Lett.* **2002**, *81*, 3191.
(41) Nakamura, S.; Iwasa, N.; Senoh, M.; Mukai, T. *Jpn. J. Appl. Phys. 1* **1992**, *31*, 1258.